

**BEM-FEM COUPLING FOR ACOUSTIC EFFECTS ON AEROELASTIC
STABILITY OF STRUCTURES**

IRTAN SAFARI

UNIVERSITI SAINS MALAYSIA

2008

**BEM-FEM COUPLING FOR ACOUSTIC EFFECTS ON AEROELASTIC
STABILITY OF STRUCTURES**

by

IRTAN SAFARI

**Thesis submitted in fulfillment of the
requirements for the degree
of Master of Science**

JULY 2008

ACKNOWLEDGEMENTS

I would like to express my sincere gratitude to Professor Harijono Djojodihardjo for his enlightening guidance, encouragement and support during the whole course of my Master study. He kindly provided me the opportunity of studying in this country and led me into the interesting world of aeroelasticity and boundary integral equations/boundary element method. By studying under his guidance and working with him closely, my knowledge of aeroelasticity and boundary integral equations/boundary element method has been greatly enriched. I am grateful for his support and giving me the opportunity to involve in many important projects: microsatellite, system dynamics and acoustic-aeroelastic projects. His encouragement, thoughtfulness, and supervision are deeply acknowledged. He will always be my guru.

I would like to thank to Dr. Radzuan Razali, Dr. Md. Adzlin Md. Said, and Dr. Setyamartana Parman for their valuable guidance, constructive ideas, and generosity in sharing their experiences.

I would like to thank my friends in ITB and USM, especially to Afiyan, Kavimani, and Parvathy for their support and encouragement. I would like to thank for their readiness when I needed their help.

Finally, I would like to express my deep appreciation to my beloved wife, Wiwin Windaningsih, for her unconditional help, sacrifice and patience and also to my beloved daughter Azka Hilyatul Aulia. I am forever grateful to my family in Limbangan, Bandung and Cirebon for their love.

TABLE OF CONTENTS

	Page
ACKNOWLEDGEMENTS	i
TABLE OF CONTENTS	ii
LIST OF TABLES	v
LIST OF FIGURES	vi
LIST OF SYMBOLS	viii
LIST OF ABBREVIATION	x
LIST OF APPENDICES	xi
LIST OF PUBLICATIONS & SEMINARS	xii
ABSTRAK	xiii
ABSTRACT	xiv
CHAPTER ONE : INTRODUCTION	
1.0 Background	1
1.1 Problem Definition	4
1.2 Objective	5
1.3 Thesis Outline	7
CHAPTER TWO : BOUNDARY ELEMENT FORMULATION	
2.0 Introduction	9
2.1 Helmholtz Integral Equation for the Acoustic Fields	9
2.2 Discretization into Boundary Element Equations	11
2.3 Implemented BEM Formulation	15
2.4 Acoustic BEM Numerical Simulation	16
2.5 Summary	19
CHAPTER THREE : FINITE ELEMENT FORMULATION	
3.0 Introduction	20
3.1 Eight Node Hexahedral Solid Element	20
3.2 Four Node Quadrilateral Shell Element	23
3.3 Implemented FEM Formulation	26
3.4 FEM Numerical Simulation	27
3.4.1 Spherical Shell	27
3.4.2 Equivalent BAH Wing	28
3.5 Summary	31
CHAPTER FOUR : COUPLED BEM-FEM FORMULATION	
4.0 Introduction	32
4.1 BEM-FEM Fluid Structure Coupling	32

4.2	Case Studies	36
4.2.1	Spherical Shell	37
4.2.2	Acoustic Excitation on Equivalent BAH Wing	39
4.3	Summary	43
CHAPTER FIVE : UNSTEADY AERODYNAMIC LOADS		
FORMULATION AND FLUTTER CALCULATION		
5.0	Introduction	45
5.1	Unsteady Aerodynamic Loads Formulation	46
5.2	Aero-Structure Coupling	51
5.3	Flutter Formulation (K-Method)	57
5.4	Unsteady Aerodynamic Loads Calculation	59
5.5	Flutter Calculation using K-Method	62
5.6	Summary	63
CHAPTER SIX : BEM-FEM ACOUSTIC-AEROELASTIC (AAC)		
FORMULATION		
6.0	Introduction	64
6.1	BEM-FEM Acoustic-Aeroelastic Coupling	64
6.2	Further Treatment for AAC; Acoustic-Aerodynamic Analogy	67
6.3	Acoustic Modified Flutter (K-Method)	70
6.4	Flutter Calculation for Coupled Unsteady Aerodynamic and Acoustic Excitation	72
6.5	AAC Parametric Study	73
6.6	Summary	75
CHAPTER SEVEN : SUMMARY AND CONCLUSIONS		
7.0	Introduction	77
7.1	Concluding Remarks	77
7.2	Future Works	80
BIBLIOGRAPHY		
APPENDICES		

LIST OF TABLES

	Page
1.1 Table 3.1: Natural Frequencies for Spherical Shell	28
1.2 Table 3.2: Typical Properties for Equivalent BAH Wing	28
1.3 Table 3.3: Five Natural Frequency for Equivalent BAH Wing Modeling with Solid Element	30
1.4 Table 3.4: Five Natural Frequency for Equivalent BAH Wing Modeling with Shell Element	31
1.5 Table 4.1: Total Acoustic Pressure Response [dB] on Equivalent BAH Wing	42

LIST OF FIGURES

	Page	
1.1	Figure 1.1: Computational Strategy for the Calculation of Acoustic Effects on Aeroelastic Stability of Structures	6
1.2	Figure 2.1: Exterior Problem for Homogenous Helmholtz Equation	10
1.3	Figure 2.2: Discretizing the Continuous Surfaces into Smaller Regions – Boundary Elements	11
1.4	Figure 2.3: Shape Function N_3 for Four Node Element	13
1.5	Figure 2.4: Four Node Linear Three Dimensional Acoustic BEM	15
1.6	Figure 2.5: Space Angle Constant C_e for a Node on a Non-Smooth Surface	16
1.7	Figure 2.6: Discretization of One Octant Pulsating Sphere	17
1.8	Figure 2.7: BEM Surface Pressure	18
1.9	Figure 2.8: Comparison of Surface Pressure on Pulsating Sphere; Exact and BEM Results	19
2.0	Figure 3.1: Eight Node Hexahedral Solid Elements	20
2.1	Figure 3.2: Four Node Quadrilateral Shell Elements	23
2.2	Figure 3.3: Discretization of Spherical Shell for FEM Modeling	27
2.3	Figure 3.4: Bending and Torsion Rigidity Curves for BAH Wing	28
2.4	Figure 3.5: Five Normal Modes Analysis for Equivalent BAH Wing Modeling with Solid Element	29
2.5	Figure 3.6: Five Normal Modes Analysis for Equivalent BAH Wing Modeling with Shell Element	30
2.6	Figure 4.1: Schematic of Fluid-Structure Interaction Domain	33
2.7	Figure 4.2: Schematic FE-BE Problem Representing Quarter Space Problem	34
2.8	Figure 4.3: Normal Displacement along the Arch Length of the Spherical Shell for $ka = 0.1$	37
2.9	Figure 4.4: Normal Displacement along the Arch Length of the Spherical Shell for $ka = 1.6$	38
3.0	Figure 4.5: Surface Pressure along the Arch Length of the Spherical Shell for $ka = 0.1$	38
3.1	Figure 4.6: Surface Pressure along the Arch Length of the Spherical Shell for $ka = 1.6$	39

3.2	Figure 4.7: Schematic FEM-BEM Problem from Whole Space to Quarter Space Domains	40
3.3	Figure 4.8: FEM-BEM Discretization	40
3.4	Figure 4.9: Incident Pressure Distribution due to Monopole Acoustic Source as an Excitation on Symmetric Equivalent BAH Wing	41
3.5	Figure 4.10: MATLAB® Discretization Representing BAH Wing Structure and its Surrounding Boundary	41
3.6	Figure 4.11: Deformation and Total Acoustic Pressure Response on Symmetric Equivalent BAH Wing	42
3.7	Figure 5.1: The Induced Velocity at Point P due to Pressure Loading on an Infinitesimal Area	47
3.8	Figure 5.2: The Lifting Surface Idealization in the Doublet Point Method	48
3.9	Figure 5.3: BAH Wing Discretization for Unsteady Aerodynamic Loads Calculation	59
4.0	Figure 5.4: Pressure Coefficient Distribution Calculated Using DPM and DLM [Real Part]	60
4.1	Figure 5.5: Pressure Coefficient Distribution Calculated Using DPM and DLM [Imaginary Part]	60
4.2	Figure 5.6: Pressure Coefficient Distribution on Section 1 Calculated Using DPM and DLM	61
4.3	Figure 5.7: Pressure Coefficient Distribution on Section 2 Calculated Using DPM and DLM	62
4.4	Figure 5.8: V-g and V-f Diagram for BAH Wing Calculated Using MATLAB® and ZAERO®	63
4.5	Figure 5.9: Unsteady aerodynamic Pressure Distribution and Mode Shape of the Wing Structure When Flutter Occurs	63
4.6	Figure 6.1: Schematic FE-BE Problem Representing Quarter Space Problem	65
4.7	Figure 6.2: Damping and Frequency Diagram for BAH Wing	72
4.8	Figure 6.3: The Influence of Monopole Acoustic Source on Flutter Velocity as a Function of Monopole Position Above Wing	73
4.9	Figure 6.4: The Influence of Monopole Acoustic Source on Flutter Velocity as a Function of Monopole Position Above Wing	74

LIST OF SYMBOLS

$[A(ik)]$	Unsteady Aerodynamics Matrix
$[A/C]$	Aerodynamics Influence Coefficient Matrix
$[C]$	Viscous Damping Matrix
$[F]$	External Forces
$[K]$	Stiffness Matrix
$[L]$	Fluid-Structure Coupling Matrix
$[M]$	Mass Matrix
$[T]$	Fluid-Structure Coupling Matrix
a	Monopole or Pulsating Sphere Radius
b	Wing Chord/Span Chosen for Convenience
c	Constant for BEM Equation, or Speed of Sound
C_p	Pressure Coefficient
f	Frequency
g	Free Space Green's Function
G	Influence Coefficient Matrix
H	Influence Coefficient Matrix
i	Field Point
j	Source Point
k	Reduced Frequency
k_w	Wave Number
N	Shape Function
n_0	Surface Unit Normal Vector
p	Total Acoustic Pressure
p_{inc}	Incident Acoustic Pressure
p_{sc}	Scattering Acoustic Pressure
q	Generalized Coordinates
q_∞	Dynamic Pressure of the Fluid Surrounding the Structure
R	Point Anywhere in Fluid Domain
R_0	Point Located on the Boundary Surface S
S	Closed Surface or Boundary
v	Normal Velocity
V_{ext}	Exterior Region in Problem Domain
V	Region on Problem Domain
Λ	Imaginary Surface

ρ Density of Material or Fluid/Gas
 δ Kronecker's Delta Function
 λ Wave Length

LIST OF ABBREVIATION

AAC	Acoustic-Aeroelastic Coupling
BAH	Bisplinghoff, Ashley, and Halfman
BE	Boundary Element
BEM	Boundary Element Method
BIE	Boundary Integral Equation
BIEM	Boundary Integral Element Method
DLM	Doublet Lattice Method
DPM	Doublet Point Method
FE	Finite Element
FEM	Finite Element Method
NASP	National Aero Space Plane

LIST OF APPENDICES

- 1.1 Appendix A: Coupling Matrix
- 1.2 Appendix B: 3D Free Space Green's Function and Normal Derivatives
- 1.3 Appendix C: Helmholtz Integral Equation for the Acoustic Field
- 1.4 Appendix D: SVD Technique and CHIEF Method for Solving Non-Uniqueness Problem in Acoustic Scattering
- 1.5 Appendix E: MATLAB Programming Code
- 1.6 Appendix F: MATLAB Programming Function Code
- 1.7 Appendix G: Exact Solution for Spherical Shell Problem

LIST OF PUBLICATIONS & SEMINARS

- 1.1 Publication A: Unified Computational Scheme For Acoustic Aeroelastomechanic Interaction
- 1.2 Publication B: BEM-FEM Coupling for Acoustic Effects on Aeroelastic Stability of Structures
- 1.3 Publication C: Parametric Studies on BEM-FEM Fluid-Structure Coupling for Acoustic Excitation on Elastic Structures
- 1.4 Publication D: Modeling and Analysis of Spacecraft Structures Subject to Acoustic Excitation

GANDINGAN BEM-FEM UNTUK KESAN AKUSTIK KEATAS KESTABILAN AEROANJALAN STRUKTUR

ABSTRAK

Satu siri kerja telah dijalankan untuk membangunkan satu asas bagi skim komputasi dalam pengiraan pengaruh gangguan akustik terhadap kestabilan aeroanjalan struktur.

Pendekatan am merangkumi tiga bahagian. Bahagian pertama adalah formulasi perambatan gelombang akustik yang ditakrifkan oleh Persamaan Helmholtz dengan menggunakan pendekatan Elemen Batas; yang membolehkan pengiraan tekanan akustik pada batas-batas akustik-struktur. Masalah dinamik struktur ini diformulasikan dengan menggunakan Kaedah Elemen Terhingga. Bahagian ketiga pula melibatkan penentuan beban aerodinamik yang tidak stabil pada struktur melalui pendekatan komputasi aerodinamik yang am.

Sepertimana masalah kestabilan aeroanjalan dinamik dilihat, kesan gangguan tekanan akustik terhadap struktur aeroanjalan dianggap merangkumi tekanan akustik insiden yang bebas daripada pergerakan struktur dan tekanan akustik yang bergantung pada pergerakan struktur. Ini ditakrifkan sebagai analogi aerodinamik akustik.

Dalam proses pembangunan ini, penumpuan teliti telah diberikan kepada masalah taburan akustik. Persamaan yang menakrifkan masalah akustik-aerodinamik ini kemudiannya telah diformulasikan dengan melingkungi tekanan total (insiden ditambah dengan tekanan tertabur), dan analogi aerodinamik akustik. Satu pendekatan am untuk menyelesaikan persamaan takrifan ini sebagai satu persamaan stabiliti telah diformulasikan untuk membolehkan pengunifikasian penyelesaian masalah ini.

BEM-FEM COUPLING FOR ACOUSTIC EFFECTS ON AEROELASTIC STABILITY OF STRUCTURES

ABSTRACT

A series of work has been carried out to develop the foundation for the computational scheme for the calculation of the influence of the acoustic disturbance to the aeroelastic stability of the structure.

The generic approach consists of three parts. The first is the formulation of the acoustic wave propagation governed by the Helmholtz equation by using boundary element approach, which then allows the calculation of the acoustic pressure on the acoustic-structure boundaries. The structural dynamic problem is formulated using finite element approach. The third part involves the calculation of the unsteady aerodynamics loading on the structure using generic unsteady aerodynamics computational method.

Analogous to the treatment of dynamic aeroelastic stability problem of structure, the effect of acoustic pressure disturbance to the aeroelastic structure is considered to consist of structural motion independent incident acoustic pressure and structural motion dependent acoustic pressure, referred to as the acoustic aerodynamic analogy.

In the present development, rigorous consideration has been devoted to the acoustic scattering problem. The governing equation for the acousto-aeroelastic problem is then formulated incorporating the total pressure (incident plus scattering pressure), and the acoustic aerodynamic analogy. A generic approach to solve the governing equation as a stability equation is formulated allowing a unified treatment of the problem.

CHAPTER ONE INTRODUCTION

1.0 Background

Aeroelasticity deals with the science that studies the mutual interaction between aerodynamic forces and elastic forces for an aerospace vehicle. One of the major research areas in the field of aeroelasticity is flutter control. Flutter is a physical phenomenon that occurs in a solid elastic structure interacting with a flow of gas or fluid. Flutter is a structural dynamical instability, which consists of violent vibrations of the solid structure with rapidly increasing amplitude. It usually results either in serious damage of the structure or in its complete destruction. Flutter occurs when the parameters characterizing fluid-structure interaction reach certain critical values. The physical reason for this phenomenon is that under special conditions, the energy of the flow is rapidly absorbed by the structure and transformed into the energy of mechanical vibrations. In engineering practice, flutter must be avoided either by design of the structure or by introducing a control mechanism capable of suppressing harmful vibrations. Flutter is known as an inherent feature of fluid-structure interaction and, thus, it cannot be eliminated completely. However, the critical conditions for flutter onset can be shifted to the safe range of the operating parameters. This is the ultimate goal for the design of flutter control mechanisms [1].

Efforts to suppress flutter could be done both passive flutter suppression (with redistribution of wing's mass and rigidity) and active flutter suppression (by actuating the control surfaces on the wing). Various active flutter suppression methods such as active control system using optimal control, adaptive control, neural networks, etc, have been implemented. But there are many other alternatives that can be implemented for flutter suppression system. One of the emerging innovations is, using sound waves as

an alternative for flutter suppression system. The idea stems from the fact that the interaction between sound and structure could create vibration.

Structure-acoustic interaction, in particular the vibration of structures due to sound waves, is a significant issue that is found in many applications. Historically, the approach to the analysis of situations embodying the interaction of vibrating elastic structures with an ambient acoustic fluid has evolved through a sequence of distinct stages. Early analytical attempts were typically motivated by practical applications. Thus the first interaction analyses were prompted by the development of underwater sound sources required for echo-ranging submerged targets, originally icebergs, after the Titanic's tragedy (1912), and then submarines 'during World War I. While interaction phenomena are generally associated with submerged structures, many of the early radiation loading studies were stimulated by the development of loudspeakers, i.e. by structures whose low structural impedance does not dwarf the light radiation loading exerted by the atmosphere.

In early 1960's an energy formulation of the acoustic-structure interaction problems has been developed, this formulation set the stage for the application of finite element methods to cavity-structure analysis. This numerical method makes the consideration of complex cavity and structure geometry, structure boundary condition, and acoustic boundary condition conceptually no more difficult than simpler problems. Three different formulations were derived using the pressure, fluid particle displacement, or velocity potential as the fundamental unknowns in the fluid region. The finite element approach for the structural-acoustic interaction problem seems well developed in 1970. As a powerful alternative to the finite element method, the boundary element method (BEM) or the boundary integral element method (BIEM) had its beginnings in the early 1960s based on the boundary integral equation theory developed in 1800s and 1900s. Most of the boundary element method applications in

acoustics focused on the acoustic radiation and scattering problems, where finite element methods have an incompatible advantage for dealing with infinite domain [2]. Due to many engineering problems which are not ideally suited for either the boundary element or finite element method, a combination of both methods seem to be the most efficient way of analysis.

Another intensive research area in acoustic-structure field is an acoustic excitation of the aircraft structure that has been one of the main concerns during certain flight operations, as exhibited by the acoustic loads on B-52 wing during take off as reported by Edson [3], which reaches acoustic sound pressure levels as high as 164 dB. Modern new and relatively lighter aircrafts may be subject to higher acoustic sound pressure level, such as predicted for the NASP [4]. Typical structural acoustic and high frequency vibration problems that can severely and adversely affect spacecraft structures and their payloads have also been lucidly described by Eaton [5]. For many classes of structures exhibiting a plate-like vibration behavior, such as antennas and solar panels, their low-order mode response is likely to be of greatest importance. Assessment of combined acoustical and quasi-static loads may be significant. The stages in the evolution of approaches to the vibrations of elastic shells and plates in an acoustic fluid and to the resulting sound field have been described by Junger [6].

Modeling of structural-acoustic interaction by using coupled BEM-FEM approaches has been attempted by many investigators such as given by Holström [7], Marquez, Meddahi, and Selgas [8] who considered two dimensional fluid-solid interaction problem, Zhang, Wu, and Lee [9] who considered acoustic radiation from bodies submerged in a subsonic non-uniform flow field, Chen, Ju, and Cha [10] who considered symmetric formulation to compute responses of submerged elastic structures in a heavy acoustic medium, Tong, Zhang, and Hua [11] who considered vibration and acoustic radiation characteristics of a submerged structure, Citarella,

Federico and Cicatiello [12] who considered vibro-acoustic analysis in automobile compartment, and Chuh Mei and Pates [13,14], who also considered the control of acoustic pressure using piezoelectric actuators by using coupled BE/FE Method. A common feature of those investigations is the joining of the boundary element method with the finite element method. The finite element method was used to model the structures, while fluid domain was handled by a boundary element method.

1.1 Problem Definition

Active flutter suppression system using sound wave can be categorized as a class of fluid-structure interaction problem. Hence the aerodynamics loads, acoustic loads and elastic structure problem must be solved simultaneously. Fluid-structure interaction should be described by a system of partial differential equations, a system that contains both the equations governing the vibrations of an elastic structure and the aerodynamic and acoustic equations governing the motion of fluid flow. The system of equations of motion should be supplied with appropriate boundary and initial conditions. The structural, aerodynamic, and acoustic parts of the system must be coupled in the following sense. The aerodynamic and acoustic equations define a pressure distribution on the elastic structure. This pressure distribution in turn defines the so-called aerodynamic and acoustic loads, which appear as forcing terms in structural equations. On the other hand, the parameters of the elastic structure enter the boundary conditions for the aerodynamic and acoustic equation.

The aerodynamic forces applied on the structure can be generally split into two parts; the external aerodynamic forces (motion independent) and motion induced aerodynamic forces. The external aerodynamic forces are usually provided, typical example are the continuous atmospheric turbulence, impulsive-type gusts, store ejection forces or control surface aerodynamic forces due to pilot's input command. The generation of motion induced aerodynamic forces normally relies on the theoretical

prediction that requires the unsteady aerodynamic computations. Since this type of forces depends on the structural deformation, the relationship can be interpreted as an aerodynamic feedback.

Analogous to the treatment of dynamic aeroelastic stability problem of structure, in which the aerodynamic effects can be distinguished into motion independent and motion induced aerodynamic forces, the effect of acoustic pressure disturbance to the aeroelastic structure (acousto-aero-elastic problem) can be viewed to consist of structural motion independent incident acoustic pressure and structural motion dependent acoustic pressure, which is known as the scattering pressure. This can be referred to as the acoustic aerodynamic analogy.

Due to the complex geometry of many structural problems, numerical methods have become the tool of choice. The finite element method (FEM) is a well established technique that offers many advantages when modeling the structure. The boundary element method (BEM) has become a popular technique when modeling acoustic domains.

1.2 Objective

The overall objective of the present study was to establish a computational procedure for the effects of acoustic disturbance to the aeroelastic stability of structure through rigorous formulation and validation and gets the overall problem solved through viable and reproducible computational routine. To perform this task, the generic approaches that consist of three parts are considered. The first part involves the formulation of the acoustic wave propagation governed by the Helmholtz equation by using boundary element approach, which then allows the calculation of the acoustic pressure on the acoustic-structure boundaries. The second part addresses the structural dynamic problem using finite element approach. The acoustic-structure

interaction is then given special attention to formulate the BEM-FEM fluid-structure coupling. The third part involves the calculation of the unsteady aerodynamic loading on the structure using a conveniently chosen unsteady aerodynamics computational method. Fig. 1.1 shows the integration strategy for the calculation of the acoustic effects on aeroelastic structure.

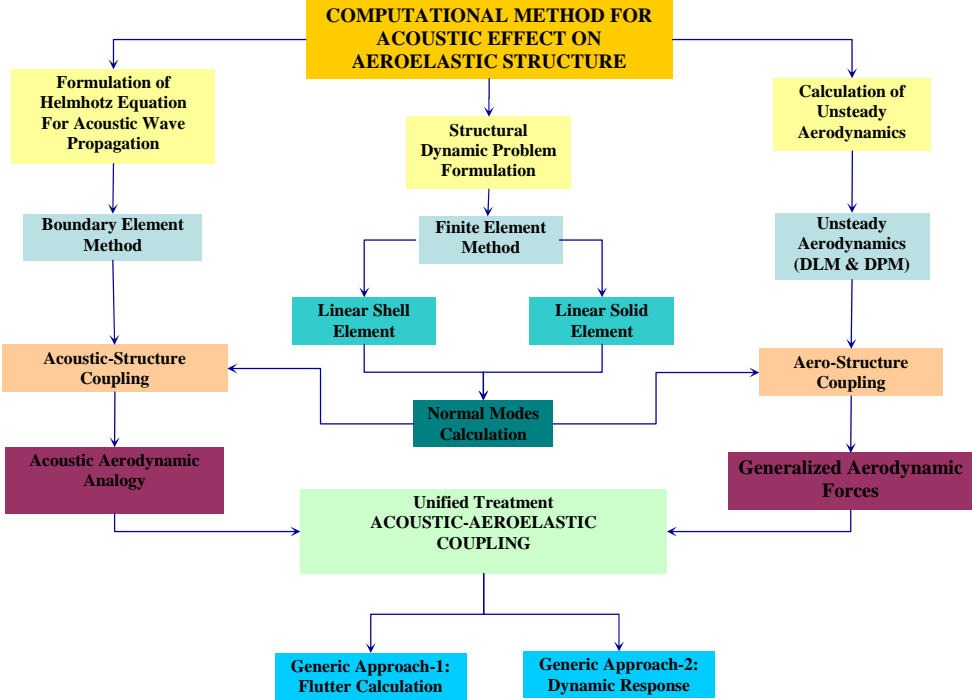


Figure 1.1: Integration strategy for the calculation of the acoustic effects on aeroelastic stability of structure

A simplified yet illustrative and instructive example has been worked out, and the computational scheme has been validated using classical results. The purpose was to develop an in-house computational scheme using MATLAB® which is considered user friendly for instructional as well as further development purposes.

1.3 Thesis Outline

Outline of this thesis will start with introduction, where the background, problem definition, and objective of this thesis are briefly discussed.

The next step is chapter two, which primarily will deal with Helmholtz integral equation for the three dimensional acoustic field. Next the discretization of Helmholtz integral equation into boundary element equations and derivation of the influence coefficient matrix \mathbf{H} and \mathbf{G} using standard procedure for iso-parametric four node quadrilateral linear boundary elements treatment are implemented. The objective is to develop and validate the boundary element method as an accurate numerical technique for acoustic domains. Some case studies to perform the correctness of the in-house developed BEM computational program written in MATLAB® are also given

Chapter three will discuss the linear finite element formulation of the structure. The objective is to acquire a finite element program to accurately model the structural system and obtain pertinent linear theory information needed to couple with the boundary element method. Some case studies to perform the correctness of the in-house developed FEM computational program written in MATLAB® are also given

Chapter four, the coupled BEM-FEM formulation representing fluid structure interaction problem will be described for structure-acoustic application. The objective involves coupling the boundary element method and the finite element method to model the total coupled system. Some case studies to perform the correctness of the in-house developed coupled BEM-FEM computational program written in MATLAB® are also given.

Chapter five, the unsteady aerodynamic loads formulation using Doublet Point Method (DPM), aero-structure coupling and flutter calculation using K-method will be

described for structure-acoustic application. The objective is to develop and validate the unsteady aerodynamic loads calculation (DPM) and flutter calculation using K-Method as an accurate numerical computational routine for further utilization in acoustic-aeroelastic stability calculation. Some case studies to perform the correctness of the in-house developed unsteady aerodynamic computational program as well as flutter calculation using K-Method written in MATLAB® are also given

Subsequently in chapter six, BEM-FEM acoustic-aeroelastic (AAC) coupling representing acoustic-aerodynamic-structure interaction problem will be described for the calculation of the influence of the acoustic disturbance to the aeroelastic stability of the structure application. The objective involves coupling the boundary element method and the finite element method for acoustic-structure interaction and incorporating aero-structure coupling to model the total coupled system. Some case studies to perform the correctness of the in-house developed BEM-FEM acoustic-aeroelastic coupling (AAC) computational program written in MATLAB® are also given.

Chapter seven finally serves as the summary and conclusions chapter, whereby the essence of this thesis is succinctly revisited to conclude the works that has been retained, and where further refinement of the method is proposed for further works in the future.

CHAPTER TWO

BOUNDARY ELEMENT FORMULATION

2.0 Introduction

In this chapter, Helmholtz integral equation for the three dimensional acoustic field is considered. Next the discretization of Helmholtz integral equation into boundary element equations and derivation of the influence coefficient matrix H and G using standard procedure for iso-parametric four node quadrilateral linear boundary elements treatment are implemented. The objective is to develop and validate the boundary element method as an accurate numerical technique for acoustic domains. Some case studies to perform the correctness of the in-house developed BEM computational program written in MATLAB® are also given.

The Boundary Element Method (BEM) is a numerical analysis technique used to obtain solutions to the partial differential equations of a variety of physical problems with well defined boundary conditions [15]. The differential equation, which is defined over the entire problem domain, is transformed into a surface integral equation over the surfaces that enclosed entirely the problem domain. The surface integral equation can then be solved by discretizing the surfaces into smaller regions - boundary elements. A major advantage of the boundary element method over the finite element method is that the discretization occurs only on the surfaces rather than over the entire domain, and the number of boundary elements required is generally a lot less than the number of finite elements required. This is particularly advantageous for acoustic applications where the problem domain often involves the entire three dimensional spaces in free field.

2.1 Helmholtz Integral Equation for the Acoustic Field

For an exterior acoustic problem, as depicted in Fig. 2.1, the problem domain V is the free space V_{ext} outside the closed surface S . V is considered enclosed in between the surface S and an imaginary surface A at a sufficiently large distance from the acoustic sources and the surface S such that the boundary condition on A satisfies Sommerfeld's acoustic radiation condition as the distance approaches infinity.

For time-harmonic acoustic problems in fluid domains, the corresponding boundary integral equation is the Helmholtz integral equation [16].

$$cp(R) = \int_S \left(p(R) \frac{\partial g}{\partial n_0} - g(|R - R_0|) \frac{\partial p}{\partial n_0} \right) dS \quad (2.1)$$

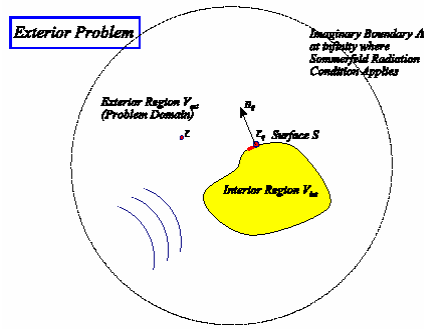


Figure 2.1: Exterior problem for homogeneous Helmholtz equation

where n_0 is the surface unit normal vector, and the value of c depends on the location of R in the fluid domain, and where g the free-space Green's function. R_0 denote a point located on the boundary S , as given by

$$g(|R - R_0|) = \frac{e^{-ik|R - R_0|}}{4\pi|R - R_0|} \quad (2.2)$$

To solve Eq. (2.1) with g given by Eq. (2.2), one of the two physical properties, acoustic pressure and normal velocity, must be known at every point on the boundary surface. At the infinite boundary A , the Sommerfeld radiation condition in three dimensions can be written as [16]:

$$\lim_{|R-R_0| \rightarrow \infty} r \left(\frac{\partial g}{\partial r} + ikg \right) \Rightarrow 0 \quad \text{as } r \Rightarrow \infty, r = |R - R_0| \quad (2.3)$$

which is satisfied by the fundamental solution.

The total pressure, which consists of incident and scattering pressure, serves as an acoustic excitation on the structure. The integral equation for the total wave is given by

$$cp(R) - p_{inc}(R) = \int_S \left[p(R) \frac{\partial g(R-R_0)}{\partial n_0} - \frac{\partial p(r)}{\partial n_0} g(R-R_0) \right] dS \quad (2.4)$$

where $p = p_{inc} + p_{scattering}$, and where

$$c = \begin{cases} 1 & , R \in V_{ext} \\ 1/2 & , R \in S \\ \Omega/4\pi & , R \in S \text{ (non smooth surface)} \\ 0 & , R \in V_{int} \end{cases} \quad (2.5)$$

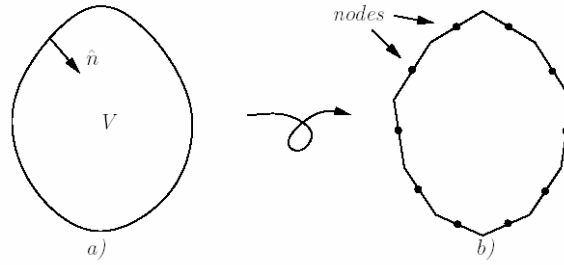


Figure 2.2: Discretizing the continuous surfaces a) into smaller regions - boundary elements b)

2.2 Discretization into BE Equations

The Helmholtz equation is then discretized by dividing the boundary surface S into N elements as depicted in Fig.2.2. The discretized boundary integral equation becomes,

$$cp_i - p_{inc} - \sum_{j=1}^N \int_S \bar{p}_j g dS = i \rho_0 \omega \sum_{j=1}^N \int_S g v_j dS \quad (2.6)$$

where i indicates field point, j source point and S_j surface element j , and for convenience, \bar{g} is defined as

$$\bar{g} \equiv \frac{\partial g}{\partial n} \quad (2.7)$$

Let

$$\bar{H}_{ij} = \int_{S_j} \bar{g} dS \quad (2.8), \quad G_{ij} = \int_{S_j} g dS \quad (2.9)$$

Substituting g in Eq. (2.2) to be the monopole Green's free-space fundamental solution, it follows that:

$$G_{ij} = \int_S g dS = \int_S g(|R_j - R_i|) dS = \int_S \frac{e^{-ik(|R_j - R_i|)}}{4\pi(|R_j - R_i|)} dS \quad (2.10)$$

or, in Cartesian coordinate system,

$$G_{ij} = \int_{S_j} \frac{e^{-ik\sqrt{(x_j - x_i)^2 + (y_j - y_i)^2 + (z_j - z_i)^2}}}{4\pi\sqrt{(x_j - x_i)^2 + (y_j - y_i)^2 + (z_j - z_i)^2}} dS \quad (2.11)$$

where R_j is the coordinate vector of the midpoint of element j and R_i is the coordinate vector of the node i . In the development that follows, four-node iso-parametric quadrilateral elements are used throughout. To calculate \bar{H}_{ij} , the derivative \bar{g} has to be evaluated

$$\bar{H}_{ij} = \int_{S_j} \bar{g} dS = \int_{S_j} \frac{\partial g}{\partial \hat{n}} dS = \int_{S_j} (\nabla g)^T \hat{n} dS \quad (2.12)$$

where

$$\hat{n} = \begin{bmatrix} n_x \\ n_y \\ n_z \end{bmatrix} \quad (2.13)$$

and

$$\nabla g = \begin{bmatrix} -\frac{xe^{-ik\sqrt{(x_i-x_j)^2+(y_i-y_j)^2+(z_i-z_j)^2}}}{4\pi\sqrt{(x_i-x_j)^2+(y_i-y_j)^2+(z_i-z_j)^2}} \left(ik + \frac{1}{\sqrt{(x_i-x_j)^2+(y_i-y_j)^2+(z_i-z_j)^2}} \right) \\ -\frac{ye^{-ik\sqrt{(x_i-x_j)^2+(y_i-y_j)^2+(z_i-z_j)^2}}}{4\pi\sqrt{(x_i-x_j)^2+(y_i-y_j)^2+(z_i-z_j)^2}} \left(ik + \frac{1}{\sqrt{(x_i-x_j)^2+(y_i-y_j)^2+(z_i-z_j)^2}} \right) \\ -\frac{ze^{-ik\sqrt{(x_i-x_j)^2+(y_i-y_j)^2+(z_i-z_j)^2}}}{4\pi\sqrt{(x_i-x_j)^2+(y_i-y_j)^2+(z_i-z_j)^2}} \left(ik + \frac{1}{\sqrt{(x_i-x_j)^2+(y_i-y_j)^2+(z_i-z_j)^2}} \right) \end{bmatrix} \quad (2.14)$$

For a four-node iso-parametric quadrilateral element, the pressure p and the normal velocity v at any position on the element can be defined by their nodal values and linear shape functions, i.e.

$$v(\xi, \eta) = N_1 v_1 + N_2 v_2 + N_3 v_3 + N_4 v_4 = [N_1 \quad N_2 \quad N_3 \quad N_4] \begin{bmatrix} v_1 \\ v_2 \\ v_3 \\ v_4 \end{bmatrix} \quad (2.15)$$

$$p(\xi, \eta) = N_1 p_1 + N_2 p_2 + N_3 p_3 + N_4 p_4 = [N_1 \quad N_2 \quad N_3 \quad N_4] \begin{bmatrix} p_1 \\ p_2 \\ p_3 \\ p_4 \end{bmatrix} \quad (2.16)$$

where the shape functions in the element coordinate system as depicted in Fig. 2.3 are,

$$\begin{aligned} N_1 &= \frac{1}{4}(\xi-1)(\eta-1) & N_2 &= -\frac{1}{4}(\xi+1)(\eta-1) \\ N_3 &= \frac{1}{4}(\xi+1)(\eta+1) & N_4 &= -\frac{1}{4}(\xi-1)(\eta+1) \end{aligned} \quad (2.17)$$

The four node quadrilateral element can have any arbitrary orientation in the three-dimensional space. Using the shape functions (2.17), the integral on the left hand side of Eq. (2.6), considered over one element j , can be written as:

$$\int_{S_j} p \bar{g}_i ds = \int_{S_j} [N_1 \quad N_2 \quad N_3 \quad N_4] \bar{g}_i dS \begin{bmatrix} p_1 \\ p_2 \\ p_3 \\ p_4 \end{bmatrix}_j = \begin{bmatrix} \bar{h}_{ij}^1 & \bar{h}_{ij}^2 & \bar{h}_{ij}^3 & \bar{h}_{ij}^4 \end{bmatrix} \begin{bmatrix} p_1 \\ p_2 \\ p_3 \\ p_4 \end{bmatrix}_j \quad (2.18)$$

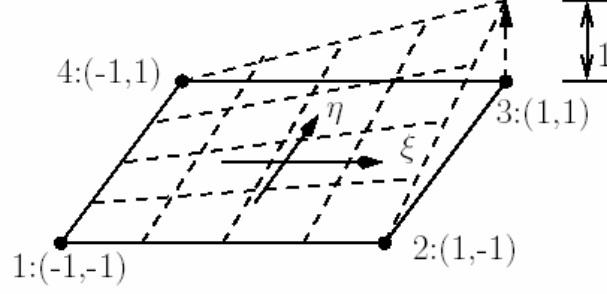


Figure 2.3: Shape function N3 for a four node elements

while that on the right hand side

$$\int_{S_j} g v dS = \int_{S_j} [N_1 \quad N_2 \quad N_3 \quad N_4] g_i dS \begin{bmatrix} v_1 \\ v_2 \\ v_3 \\ v_4 \end{bmatrix}_j = [g_{ij}^1 \quad g_{ij}^2 \quad g_{ij}^3 \quad g_{ij}^n] \begin{bmatrix} v_1 \\ v_2 \\ v_3 \\ v_4 \end{bmatrix}_i \quad (2.19)$$

where

$$\bar{h}_{ij}^k = \int_{S_j} N_k \bar{g}_j dS \quad k = 1, 2, 3, 4 \quad (2.20)$$

$$g_{ij}^k = \int_{S_j} N_k g_j dS \quad k = 1, 2, 3, 4 \quad (2.21)$$

The integration in Eq. (2.18) and (2.19) can be carried out using Gauss points [7,17].

These Gauss points in the iso-parametric system are defined as:

$$\begin{aligned} (\xi_1, \eta_1) &= \frac{1}{\sqrt{3}}(1, -1) & (\xi_2, \eta_2) &= \frac{1}{\sqrt{3}}(1, 1) \\ (\xi_3, \eta_3) &= \frac{1}{\sqrt{3}}(-1, 1) & (\xi_4, \eta_4) &= \frac{1}{\sqrt{3}}(-1, -1) \end{aligned} \quad (2.22)$$

Substituting equations (2.18) and (2.19) into equation (2.6) for all elements j , there is obtained

$$c_i \rho_i - \rho_{inc} - \sum_{j=1, j \neq i}^N [\bar{h}_{ij}^1 \quad \bar{h}_{ij}^2 \quad \bar{h}_{ij}^3 \quad \bar{h}_{ij}^4] \begin{bmatrix} \rho_1 \\ \rho_2 \\ \rho_3 \\ \rho_4 \end{bmatrix}_j = i \rho \omega_0 \sum_{j=1}^N [g_{ij}^1 \quad g_{ij}^2 \quad g_{ij}^3 \quad g_{ij}^4] \begin{bmatrix} v_{n1} \\ v_{n2} \\ v_{n3} \\ v_{n4} \end{bmatrix}_j \quad (2.23)$$

Equation (2.23) can be rewritten as

$$\sum_{j=1}^N \begin{bmatrix} h^1_{ij} & h^2_{ij} & h^3_{ij} & h^4_{ij} \end{bmatrix} \begin{bmatrix} p_1 \\ p_2 \\ p_3 \\ p_4 \end{bmatrix}_j = i\rho\omega_0 \sum_{j=1}^N \begin{bmatrix} g^1_{ij} & g^2_{ij} & g^3_{ij} & g^4_{ij} \end{bmatrix} \begin{bmatrix} v_{n1} \\ v_{n2} \\ v_{n3} \\ v_{n4} \end{bmatrix}_j + p_{inc} \quad (2.24)$$

The discretized equation forms a set of simultaneous linear equations, which relates the pressure p_i at field point i due to the boundary conditions p to v at source surface S_i of element i and the incident pressure p_{inc} . In matrix form:

$$[\mathbf{H}]\{p\} = i\rho_0\omega[\mathbf{G}]\{v\} + \{p_{inc}\} \quad (2.25)$$

where, \mathbf{H} and \mathbf{G} are two $N \times N$ matrices of influence coefficients, while p and v are vectors of dimension N representing total pressure and normal velocity on the boundary elements. This matrix equation can be solved if the boundary condition $v = \partial p / \partial n$ and the incident acoustic pressure field p_{inc} are known.

2.3 Implemented BEM Formulation

Based on the BEM formulation for four node iso-parametric quadrilateral linear acoustic elements, a computational routine written in MATLAB® have been developed and implemented in order to solve BEM problems for time-harmonic acoustic fluid domains. The programs routine can be described in the following steps:

- The element discretization is supplied by using commercial meshing software such as PATRAN®.

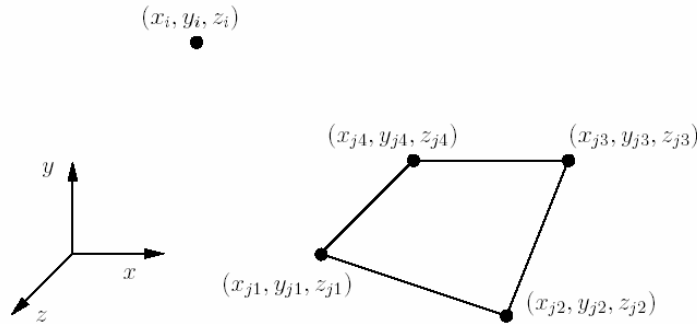


Figure 2.4: Four node linear three dimensional acoustic boundary element j , that is influencing a node located at R_i

- Compute the influence vectors **He** and **Ge** for each four node linear three dimensional acoustic boundary element j , that is influencing a node located at $R_i = (x_i, y_i, z_i)$ as shown in Fig. 2.4.
- Compute the space angle constant for a node on a non-smooth surface. For a node coinciding with three or four element corners, the space angle constant C_e is the quotient of $\Omega/4\pi$ and it's towards the acoustic medium as shown in Fig. 2.5. The space angle for a sphere is 4π and for smooth surface the space angle is 2π , and $C_e = 1$.
- Assembly all local element influence matrix H_e and G_e into the global influence matrix H and G according to each degree of freedom.
- Solve the acoustic BEM equations by adding the known prescribed physical boundary condition (pressure, normal velocity or impedance), the output are vectors providing the node boundary pressure and/or the node normal velocity.
- Compute induced acoustic pressure at an arbitrary point in a three dimensional fluid domain.

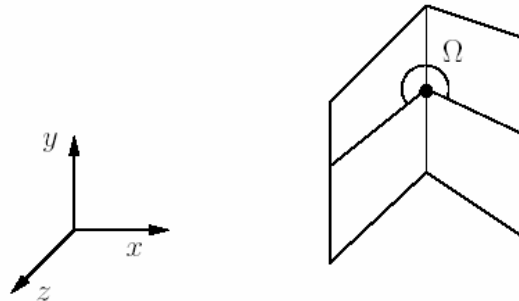


Figure 2.5: Space angle constant C_e for a node on a non-smooth surface

2.4 Acoustic BEM Numerical Simulation

In order to verify the correctness of the developed boundary elements acoustic formulation, a numerical test case is conducted to test the validity of the method. To avoid complexity, the assumed acoustic source, is monopole source which creates the acoustic pressure. For a pulsating sphere an exact solution for acoustic pressure p at a

distance r from the center of a sphere with radius a pulsating with uniform radial velocity U_a is

$$p(r) = \frac{a}{r} U_a \frac{iz_0 ka}{1 + ika} e^{-ik(r-a)} \quad (2.26)$$

where z_0 is the acoustic characteristic impedance of the medium and k is the wave number.

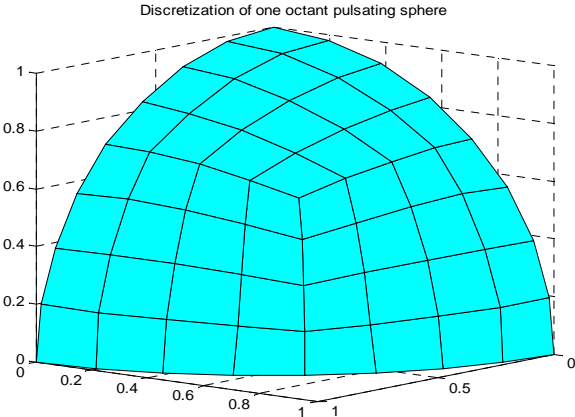
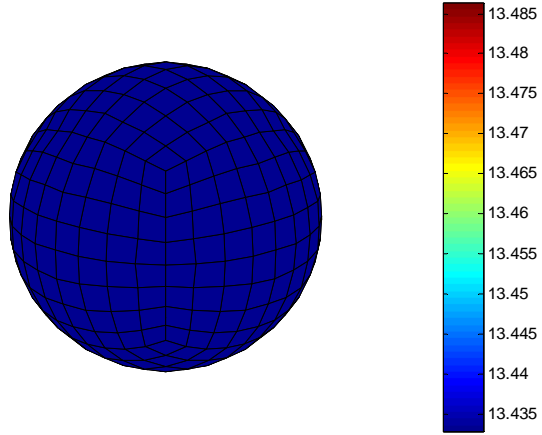


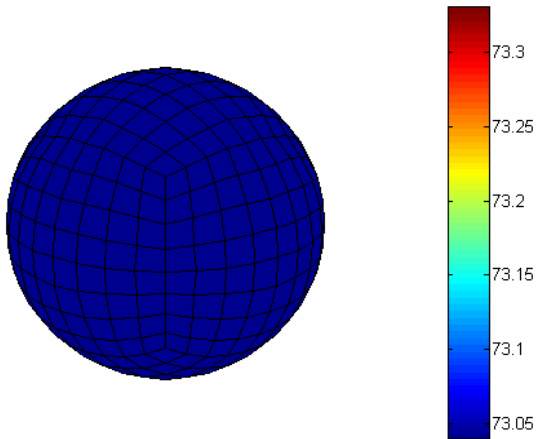
Figure 2.6: Discretization of one octant pulsating sphere

Fig. 2.6 shows the discretization of the surface elements of an acoustics pulsating sphere representing a monopole source. BEM calculation for scattering pressure from acoustic monopole source will be compared with exact results. The results are exhibited in Fig.2.7 where the calculated surface pressures on the pulsating sphere are shown. The calculation was based on the assumption of $f=10$ Hz, $\rho=1.225$ Kg/m³, and $c=340$ m/s which shows the excellent agreement between the computational procedure developed and the exact one. In Fig. 2.8, the excellent agreement of BEM calculation for acoustic pressures anywhere in three dimensional fluid domains with exact calculation serves to validate the developed MATLAB® program for further utilization.

Pressure distribution of pulsating sphere BEM [real part]



Pressure distribution of pulsating sphere BEM [imag part]



Pressure distribution of pulsating sphere BEM [magnitude]

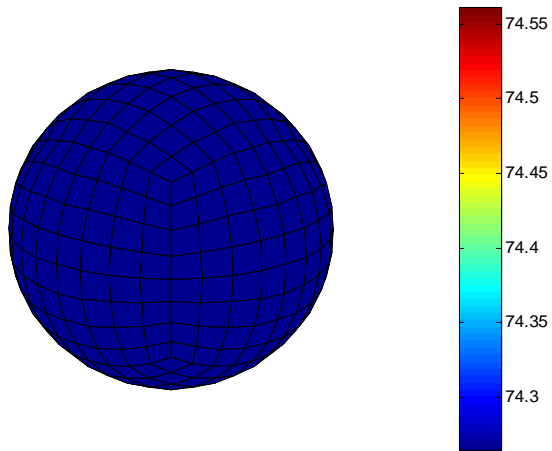


Figure 2.7: BEM surface pressure [Real, Imaginary, and Magnitude]

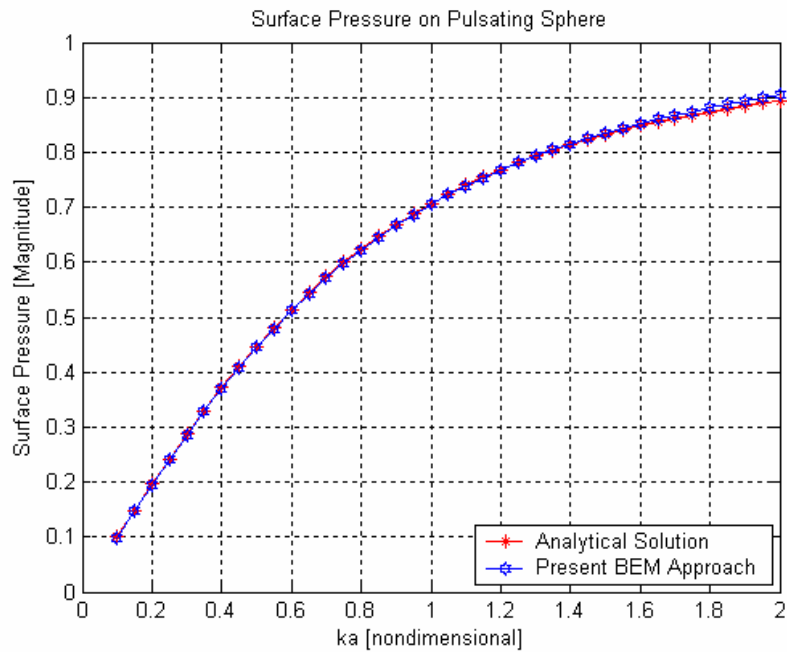


Figure 2.8: Comparison of surface pressure on pulsating sphere; exact and BEM results

2.5 Summary

The excellent agreement of BEM calculation for acoustic pressures in three dimensional fluid domains with exact calculation has been carried out and a computational scheme for acoustic boundary element problem has given satisfactory results. Hence, the objective to develop and validate the boundary element method as an accurate numerical technique for acoustic domains has been accomplished and serves to validate the in-house developed BEM computational program written in MATLAB® for further utilization.

CHAPTER THREE FINITE ELEMENT FORMULATION

3.0 Introduction

In this chapter, linear finite element formulation of the structure is described. The objective is to acquire a finite element program to accurately model the structural system and obtain pertinent linear theory information needed to couple with the boundary element method. Some case studies to perform the correctness of the in-house developed FEM computational program written in MATLAB® are also given.

The finite element method has become a very powerful tool in analyzing static and dynamic response of structures. The finite element method is capable of handling complex structural analysis. Many rectangular and triangular type finite elements are currently being used in commercial and in-house codes. Any type of finite element can be applied to the following formulation. Two elements selected for this study are considered here; these are an eight node hexahedral for solid element modeling and four node quadrilateral for shell element modeling. The FEM formulation on this chapter is mostly based on Weaver and Johnston [17]. For convenience in further reference and development, as well as for completeness, these formulations are summarized in the following sections.

3.1 Eight node hexahedral solid elements

Formulations for iso-parametric hexahedral linear solid elements with three translational degrees of freedom (DOF) per node are considered.

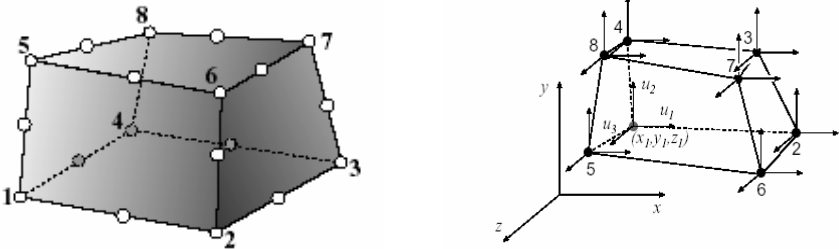


Figure 3.1: Eight node hexahedral solid elements

Nodal quantities will be identified by the node subscript. Thus $\{x_i, y_i, z_i\}$ denote the node coordinates of the i^{th} node, while $\{u_{xi}, u_{yi}, u_{zi}\}$ are the nodal displacement DOFs. The shape function for the i^{th} node is denoted by N_i . The element geometry is described by:

$$\begin{bmatrix} 1 \\ x \\ y \\ z \end{bmatrix} = \begin{bmatrix} 1 & 1 & \dots & 1 \\ x_1 & x_2 & \dots & x_n \\ y_1 & y_2 & \dots & y_n \\ z_1 & z_2 & \dots & z_n \end{bmatrix} \begin{bmatrix} N_1 \\ N_2 \\ \vdots \\ N_n \end{bmatrix} \quad (3.1)$$

The four rows of this matrix relation express the geometric conditions which the shape functions must identically satisfy.

$$1 = \sum_{i=1}^n N_i \quad x = \sum_{i=1}^n x_i N_i \quad y = \sum_{i=1}^n y_i N_i \quad z = \sum_{i=1}^n z_i N_i \quad (3.2)$$

The first one: sum of shape functions must be unity, is an essential part of the verification of completeness. The displacement interpolation is

$$\begin{bmatrix} u_x \\ u_y \\ u_z \end{bmatrix} = \begin{bmatrix} u_{x1} & u_{x2} & \dots & u_{xn} \\ u_{y1} & u_{y2} & \dots & u_{yn} \\ u_{z1} & u_{z2} & \dots & u_{zn} \end{bmatrix} \begin{bmatrix} N_1 \\ N_2 \\ \vdots \\ N_n \end{bmatrix} \quad (3.3)$$

The three rows of this matrix relation express the interpolation conditions

$$u_x = \sum_{i=1}^n u_{xi} N_i \quad u_y = \sum_{i=1}^n u_{yi} N_i \quad u_z = \sum_{i=1}^n u_{zi} N_i \quad (3.4)$$

The identical structure of the geometry definition and displacement interpolation characterizes an iso-parametric element. The interpolation functions for eight node solid element are:

$$\begin{aligned} N_1^e &= \frac{1}{8}(1-\xi)(1-\eta)(1-\zeta) & N_5^e &= \frac{1}{8}(1-\xi)(1-\eta)(1+\zeta) \\ N_2^e &= \frac{1}{8}(1+\xi)(1-\eta)(1-\zeta) & N_6^e &= \frac{1}{8}(1+\xi)(1-\eta)(1+\zeta) \\ N_3^e &= \frac{1}{8}(1+\xi)(1+\eta)(1-\zeta) & N_7^e &= \frac{1}{8}(1+\xi)(1+\eta)(1+\zeta) \\ N_4^e &= \frac{1}{8}(1-\xi)(1+\eta)(1-\zeta) & N_8^e &= \frac{1}{8}(1-\xi)(1+\eta)(1+\zeta) \end{aligned} \quad (3.5)$$

We restrict attention to linear elastostatic analysis without initial stresses. For a general solid element the proportional matrix can be presented as:

$$D = \frac{E}{(1-\nu)(1-2\nu)} \begin{bmatrix} 1-\nu & \nu & \nu & 0 & 0 & 0 \\ \nu & 1-\nu & \nu & 0 & 0 & 0 \\ \nu & \nu & 1-\nu & 0 & 0 & 0 \\ 0 & 0 & 0 & \frac{(1-2\nu)}{2} & 0 & 0 \\ 0 & 0 & 0 & 0 & \frac{(1-2\nu)}{2} & 0 \\ 0 & 0 & 0 & 0 & 0 & \frac{(1-2\nu)}{2} \end{bmatrix} \quad (3.6)$$

The strains are related to the element node displacements by

$$\mathbf{B} = \nabla \mathbf{N}^e \quad (3.7)$$

where

$$\nabla = \begin{bmatrix} \frac{\partial}{\partial x} & 0 & 0 \\ 0 & \frac{\partial}{\partial y} & 0 \\ 0 & 0 & \frac{\partial}{\partial z} \\ \frac{\partial}{\partial y} & \frac{\partial}{\partial x} & \\ \frac{\partial}{\partial z} & & \frac{\partial}{\partial x} \\ & \frac{\partial}{\partial z} & \frac{\partial}{\partial y} \end{bmatrix}, \quad \begin{bmatrix} \frac{\partial}{\partial x} \\ \frac{\partial}{\partial y} \\ \frac{\partial}{\partial z} \end{bmatrix} = (\mathbf{J}^T)^{-1} \begin{bmatrix} \frac{\partial}{\partial \xi} \\ \frac{\partial}{\partial \eta} \\ \frac{\partial}{\partial \zeta} \end{bmatrix}, \quad \mathbf{J} = \begin{bmatrix} \frac{\partial x}{\partial \xi} & \frac{\partial x}{\partial \eta} & \frac{\partial x}{\partial \zeta} \\ \frac{\partial y}{\partial \xi} & \frac{\partial y}{\partial \eta} & \frac{\partial y}{\partial \zeta} \\ \frac{\partial z}{\partial \xi} & \frac{\partial z}{\partial \eta} & \frac{\partial z}{\partial \zeta} \end{bmatrix} \quad (3.8)$$

and for deriving the consistent mass matrix the interpolation function is rearranged as

$$\begin{bmatrix} u_x \\ u_y \\ u_z \end{bmatrix} = \begin{bmatrix} N_1 & 0 & 0 & \dots & N_8 & 0 & 0 \\ 0 & N_1 & 0 & \dots & 0 & N_8 & 0 \\ 0 & 0 & N_1 & \dots & 0 & 0 & N_8 \end{bmatrix} \begin{bmatrix} u_1 \\ u_2 \\ \vdots \\ u_{24} \end{bmatrix} \quad (3.9)$$

The element stiffness and mass matrix is formally given by the volume integral where the integral is taken over the element volume.

$$\mathbf{K}^e = \int_{V^e} \mathbf{B}^T \mathbf{D} \mathbf{B} dV \quad (3.10)$$

and

$$\mathbf{M}^e = \int_{V^e} \rho \mathbf{N}^T \mathbf{N} dV \quad (3.11)$$

By applying gauss integration the element stiffness and mass matrix became:

$$\mathbf{K} = \int_{-1}^1 \int_{-1}^1 \int_{-1}^1 \mathbf{B}^T(\xi, \eta, \zeta) \mathbf{D} \mathbf{B}(\xi, \eta, \zeta) |\mathbf{J}(\xi, \eta, \zeta)| d\xi d\eta d\zeta$$

$$\mathbf{K} = \sum_{l=1}^n \sum_{k=1}^n \sum_{j=1}^n R_j R_k R_l \mathbf{B}_{j,k,l}^T \mathbf{D} \mathbf{B}_{j,k,l} |\mathbf{J}_{j,k,l}| \quad (3.12)$$

and

$$\mathbf{M} = \int_{-1}^1 \int_{-1}^1 \int_{-1}^1 \rho \mathbf{N}^T(\xi, \eta, \zeta) \mathbf{N}(\xi, \eta, \zeta) |\mathbf{J}(\xi, \eta, \zeta)| d\xi d\eta d\zeta$$

$$\mathbf{M} = \sum_{l=1}^n \sum_{k=1}^n \sum_{j=1}^n \rho R_j R_k R_l \mathbf{N}_{j,k,l}^T \mathbf{N}_{j,k,l} |\mathbf{J}_{j,k,l}| \quad (3.13)$$

3.2 Four node quadrilateral shell elements

Formulations for Iso-parametric four node quadrilateral linear shell elements with three translational and two rotational degrees of freedom (DOF) per node are considered.

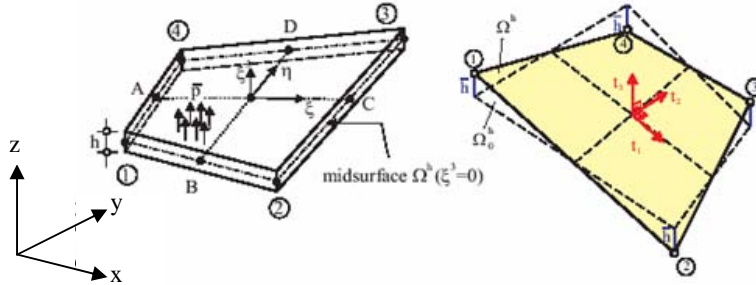


Figure 3.2: Four node quadrilateral shell elements

For a general shell element the proportional matrix can be presented as:

$$D = \frac{E}{(1-\nu^2)} \begin{bmatrix} 1 & \nu & 0 & 0 & 0 \\ \nu & 1 & 0 & 0 & 0 \\ 0 & 0 & \frac{1-\nu}{2k} & 0 & 0 \\ 0 & 0 & 0 & \frac{1-\nu}{2k} & 0 \\ 0 & 0 & 0 & 0 & \frac{1-\nu}{2k} \end{bmatrix} \quad (3.14)$$

The displacement in the shell can be written in the terms of nodal generalized displacements as:

$$\begin{bmatrix} u_x \\ u_y \\ u_z \end{bmatrix} = \sum N_i \begin{bmatrix} u_{xi} \\ u_{yi} \\ u_{zi} \end{bmatrix} - \sum N_i \frac{t}{2} \zeta \mathbf{v}_{2i} \theta_{1i} + \sum N_i \frac{t}{2} \zeta \mathbf{v}_{1i} \theta_{2i} \quad (3.15)$$

Vector \mathbf{v}_1 and \mathbf{v}_2 are determined in the following way; let \mathbf{v}_3 be the unit vector along the thickness of the shell, then:

$$\begin{aligned} \mathbf{v}_1 &= \mathbf{v}_3 \times \mathbf{v}_y \\ \mathbf{v}_2 &= \mathbf{v}_1 \times \mathbf{v}_3 \end{aligned} \quad (3.16)$$

where \mathbf{v}_3 is the unit vector in the y direction.

The interpolation functions for four node shell element are:

$$\begin{aligned} N_1^e &= \frac{1}{4}(1-\xi)(1-\eta) & N_3^e &= \frac{1}{4}(1+\xi)(1+\eta) \\ N_2^e &= \frac{1}{4}(1+\xi)(1-\eta) & N_4^e &= \frac{1}{4}(1-\xi)(1+\eta) \end{aligned} \quad (3.17)$$

and the displacement interpolation function is given by

$$\begin{bmatrix} u_x \\ u_y \\ u_z \\ \theta_x \\ \theta_y \end{bmatrix} = \begin{bmatrix} 1 & 0 & 0 & -\zeta \frac{t_i}{2} l_{2i} & -\zeta \frac{t_i}{2} l_{1i} \\ 0 & 1 & 0 & -\zeta \frac{t_i}{2} m_{2i} & -\zeta \frac{t_i}{2} m_{1i} \\ 0 & 0 & 1 & -\zeta \frac{t_i}{2} n_{2i} & -\zeta \frac{t_i}{2} n_{1i} \end{bmatrix} [N_i] \begin{Bmatrix} u_1 \\ u_1 \\ \vdots \\ u_{24} \end{Bmatrix} \quad (3.18)$$

Differentiating N to x, y, z coordinate

$$\begin{bmatrix} \frac{\partial N_i}{\partial x} \\ \frac{\partial N_i}{\partial y} \\ \frac{\partial N_i}{\partial z} \end{bmatrix} = [\mathbf{J}]^{-1} \begin{bmatrix} \frac{\partial N_i}{\partial \xi} \\ \frac{\partial N_i}{\partial \eta} \\ \frac{\partial N_i}{\partial \zeta} \end{bmatrix} \quad (3.19)$$

The strains are related to the element node displacements by